

5 Multi-Sensory Technology and Evaluation of Cognitive Mechanisms

5-1 Investigation of Hardness Perception and Development of Portable Haptic Device

NAKAYAMA Koichi and ANDO Hiroshi

We are aiming at developing a portable haptic device, as a part of research on Ultra-realistic communications system. This paper describes the study on hardness perception of human fingers in order to find required system performance for haptic devices that can render hard objects. It also describes the development of the portable haptic device.

Keywords

Portable haptic device, Hardness perception, Device development, Psychophysical experiment

1 Introduction

At the Universal Media Research Center, we aim to develop highly realistic communications with distant locations not only through sight, sound and smell but also “touch” (Fig. 1). The Multi Modal Communications Group is also in the process of creating a large-scale glasses-free 3D display^[1] (Fig. 2). However, due to the size restrictions of the display it is difficult for desktop haptic devices such as the PHANTOM^[2] and SPIDAR^[3] to provide the perception of controlling virtual objects projecting from a large-scale screen. The purpose of this research is to create a hand held portable haptic device which provides haptic information to user’s finger tips at any position of large-scale 3D images (Fig. 3).

In order to make this device a reality, this research needs to address the following issues.

<Issue 1: Defining the hardness

discriminability of objects>

In order to achieve the perception of hold-

ing a virtual object, it is necessary to provide the user with a sense of the hardness of the object. However, previous research on haptic devices has not clarified the threshold discriminating hardness (hereinafter referred to as “difference threshold”) or the minimum intensity variation ratio that can sense the differences of hardness (hereinafter referred to as “Weber ratio”). Consequently, there is a need to define the capability of differentiating the hardness of objects and clarify the required performance of haptic devices to display hard objects.

<Issue 2: Developing a portable haptic device>

Most devices that display arbitrarily-prescribed hardness are desk-top type devices^{[2][3]} and most portable devices such as three-dimensional mouses and tool devices^[4] focus on switching On/Off but do not display arbitrarily-prescribed hardness. It is for this reason that we are creating a portable haptic device that both displays arbitrarily-prescribed hardness and satisfies the device performance mentioned in Issue 1.



Fig.1 Future image of ultra-realistic communications

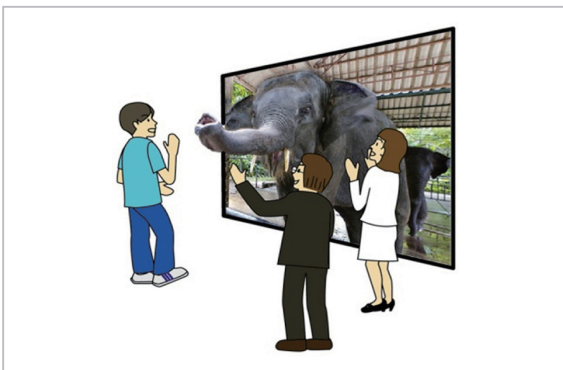


Fig.2 Future image of a high definition large-scale glasses-free 3D display

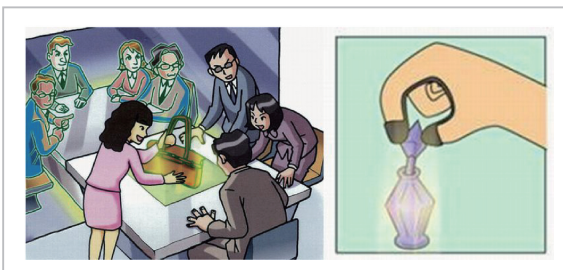


Fig.3 Future image of a portable haptic device

In order to control virtual objects displayed in 3D images, it is necessary to move such virtual objects in line with the movements of the user's hands (haptic device), not merely by displaying haptic information. Consequently, we are creating a system that provides the perception of controlling virtual objects in 3D images and developing display content that synchronizes the positional information of the haptic device and the position of the virtual objects in

3D images (Fig. 3).

Through the resolution of these two issues, users will be able to control virtual objects of varying hardness displayed in 3D images. In this paper, **2** discusses the difference threshold and the Weber ratio, **3** discusses the development of portable haptic devices mentioned in Issue 2 and **4** provides a summary of the issues discussed in this paper. Also, this paper provides additions and modifications to two journal papers (with references)[5][6], two international conferences papers (with references)[7][8], three patent applications[9]-[11] and other announcements and publications.

2 Defining hardness perception mechanics

If a person touches a real object with his/her fingers, pressure changes when the fingers that were not making contact with the object come in contact with the object. However, most haptic devices provide the sensation of touching a virtual object when the user's fingers are constantly touching the device. The finger tips perceive the change of pressure on the skin through haptic information and feel the hardness and weight of the virtual object. In addition, most haptic devices display differing pressure when touching a virtual object and do not provide the sensation of heat nor changes in the touch area of the finger tips. Consequently, the difference threshold for perceiving the differences in hardness and the Weber ratio[12], a ratio that shows the stimulation change ratio required to discriminate hardness, is thought to be different when the user touches an actual object with his/her fingers and when the user touches a virtual object with a haptic device. However, there is only a small amount of research on the difference threshold for hardness using haptic devices, and, as a result, the required control function and maximum power for displaying hardness remains unclear. Below, through the results of psychophysical experiments, we will show the difference threshold for the hardness of a rigid object using haptic devices that conveys force to the finger

tips of users.

The reason for using the difference threshold as a verification indicator is that it is not necessary to show the range of stimulation that cannot be discriminated. For example, it is not necessary for sound devices to provide sound outside an audible range or video devices to display 30 frames or more per second. Similarly, it is not necessary for haptic devices that provide a sense of holding a hard object tightly to display hardness that exceeds the difference threshold of humans.

2.1 Experimental methods

The basis of haptic information is “active touch”. This discriminates hardness through the perception of the position and speed of fingers using the somatic sense. The methods used by humans to discriminate the hardness of an object by active touch can be classified roughly into the following two patterns. The first is when hardness is discriminated through the sense of touch at the time a known object or body part lightly taps the target object, and the second pattern is when hardness is discriminated through the depth and reaction at the time the target object kneaded with the finger tips. Generally, the former is applicable to discriminating the hardness of hard objects made from substances such as metal or wood and the latter applies to discriminating the hardness of soft objects such as rubber and sponges. Even during the preliminary experiments using the PHANTOM^[2], many of the participants discriminated the hardness of an object through light tapping. Consequently, this research based on the former pattern of discriminating hardness by tapping the target object.

Experiments conducted with free active touch and without restrictions on the methods of discriminating hardness cannot be controlled since hardness may be discriminated by the varied toughing methods of the participants. Therefore, it is necessary to prevent the possibility of different difference thresholds of hardness through touch by standardizing the method of discrimination under conditions that are as close to active touch as possible.

In order to achieve this, the participants were required to discriminate hardness according to the following method. First participants imagine discriminating hardness by lightly tapping a virtual object with the rigid part of the haptic device being held by the participant (hereinafter referred to as “contact plate”). Then the participants move the contact plate as if they were lightly tapping the virtual object (hereinafter referred to as “trajectory”). Participants practice this in advance for approximately 10 minutes until they can move their fingers in line with the trajectory (maximum speed 1 m/s, stroke 100mm). After practicing these movements, the participants discriminate the hardness of a virtual object through the sensation of tapping the object with an experimental apparatus in line with the trajectory and then provide responses orally. Participants wear headphones playing loud music in order to mute the sound of the experimental apparatus and close their eyes in order to conceal the experimental apparatus during the experiment. Through this method, hardness discrimination by active touch is reproduced using the somatic sense of participants.

In addition, the experiment conducted for the purpose of this paper did not permit hardness to be discriminated using the visual and audio senses of the participants, and like the contact plate of many other haptic devices, the part of the experimental apparatus held by the fingers of participants did not allow any changes to the shape of the object (rigid body).

2.2 The experimental apparatus

The controlled motor of most haptic devices is powered by wires and gears and moves the contact plate. The controlled performance of the contact plate in haptic devices is largely affected by not only the performance of the controller that outputs control commands, but also the output performance and the control response performance of the motor that outputs power and the mechanical performance determined by the structure of the device. Consequently, in order to find the required control response performance of the contact plate, it is

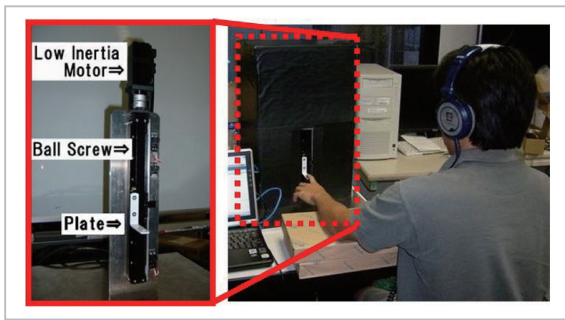


Fig.4 Overview of the experimental apparatus (left) and experimental scene (right)

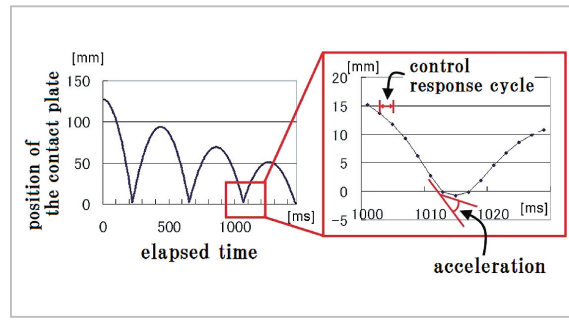


Fig.6 Trajectory of the contact plate and expanded image

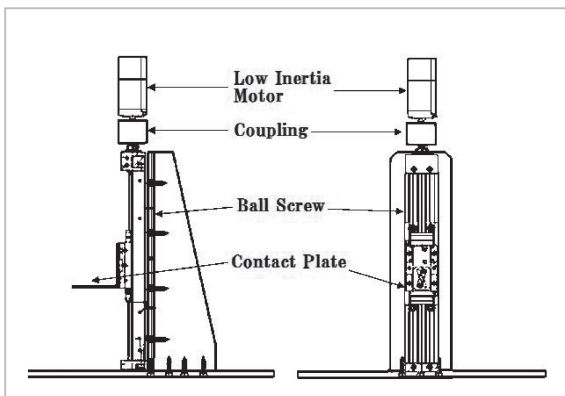


Fig.5 Structure of the experimental apparatus

necessary to consider the behavior of the contact plate including the mechanical characteristics such as deflection, strain, backlash and gear backlash (hereinafter collectively referred to as “deflection”).

This paper describes the creation of a collision haptic device that reproduces major display power and speed and a high level of control response performance after considering all the mechanical characteristics of controller performance, motor performance and the experimental apparatus. The experimental apparatus is shown on the left side and the experiment on the right side of Fig. 4. As can be seen in Fig. 4, a cover is put on the experimental device for the safety of the participant when conducting experiments. Figure 5 shows the structure of the experimental apparatus.

Although the details of the device[5] have not been included in this paper, the contact plate of the experimental apparatus has a maximum display power of 236 ~ 249N, position-

ing accuracy of $\pm 10 \mu\text{m}$, a maximum rate of acceleration of $437 \sim 462 \text{ m/s}^2$ when the contact plate is unloaded and a control response cycle of 5 ms. In addition, the position of the contact plate (behavior) can be monitored with a $\pm 10 \mu\text{m}$ margin of error through the motor encoder. Controller performance such as control command frequency in many of the existing devices has been clarified. However, the control response performance of the contact plate controlled by the communication structure is not quite as clear. This experimental apparatus can display strong power, fast acceleration, short control response cycles and small over-shoot that cannot be displayed on devices currently on the market. Furthermore, the contact plate behavior that provides actual force to the fingers of users can also be monitored with such a small margin of positional error that there is no impact on the experimental results. It is for this reason that the sensation of a collision with a hard object, a sensation which is not available on existing haptic devices, can be displayed and required performance of the contact plate examined.

2.3 Verification parameters

An example of reproducing the rebound trajectory of the contact plate that operates constant acceleration (free fall) colliding with surface of a virtual object with limited hardness using the experimental apparatus is shown in Fig. 6. The horizontal axis represents the amount of time and the vertical axis represents the position of the contact plate. Generally, the softer the virtual object the smaller the accel-

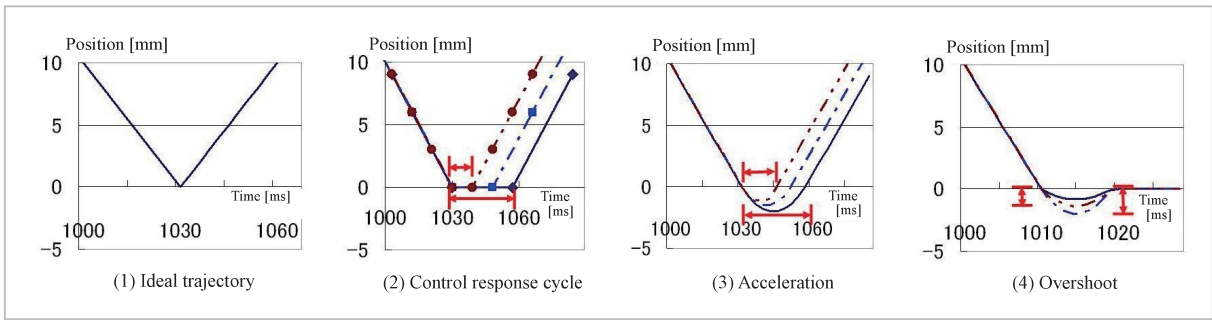


Fig.7 Four types of contact plate trajectory

eration of the rigid body (the minute length of the change of velocity received when the rigid body collided with the virtual object) and the time required from time when the rigid body makes contact with the object until the rebound (separation) is long (hereinafter referred to as “contact time”).

The right side of Fig. 6 shows an expanded image of the collision. The space between each dot shows the control command cycle and the change in the slope shows acceleration.

As shown in on the right side of Fig. 6, the contact time (the time when the distance is less than 0mm) is not necessarily equal to one control command cycle. The reason for this is that a limited time is required for the change of velocity before and after the collision due to the acceleration of the contact plate being restricted by the inertial mass of the device to the motor output. In other words, in regard to control commands, although a rebound type output is possible following one collision cycle with the object, a longer length of time than one control command cycle is required from the time such control commands are issued until the contact plate has actually rebounded. In this paper, when displaying the actual sensation of the collision, the time interval (contact time) required from the time the contact plate collides until the actual rebound is referred to as a control response cycle and discussed in distinction to the control command cycle of control commands outputted by the controller.

If one thinks of an ideal haptic device with infinite control command frequency (0 control command cycles) and infinite motor output and absolutely no deflection, as shown in Fig. 7 (1),

the contact plate trajectory will be indifferen-
tiable at the time of the collision, the control response will be zero and acceleration will be infinite. In actual fact, when control command cycles for the controller bottlenecks, the contact plate trajectory will behave as shown in Fig. 7 (2), and the command response cycle will be dependent on the control command cycle. When the motor output bottlenecks, the trajectory behaves as shown in Fig. 7 (3) and the control response cycle will be dependent on the maximum acceleration. In other words, in order to clarify the performance required for each bottleneck situation, it is necessary to examine the parameters of both the control response cycles and maximum acceleration.

At times, the contact plate of encounter-type devices that display arbitrarily curved surfaces[13] and devices that display haptic information by damping mechanisms[4][14] (hereinafter referred to as “damping mechanism-type devices”) do not rebound. When deflection is infinite, the contact plate trajectory for these types of haptic devices behaves as shown in Fig. 7 (4) and only the deflection part overshoots from the control command position. As a result, it is also necessary to examine amount of overshooting the contact plate of haptic devices can allow.

In this paper, we will examine the difference threshold of the three parameters (control response cycle/acceleration/overshoot) that indicate the haptic device performance required to display hard objects. The harder the object, the more acceleration, shorter control cycles and smaller overshoot is required.

The stimuli displayed to the participants in

each of the experiments for the three parameters are specified below. These were classified into five categories according to a geometric progression with a common ratio 2 based on the Stevens' power law^[15].

(1) Control Response Cycle

$\subset \{10, 20, 40, 80, 160(\text{ms})\}$

(2) Acceleration $\subset \{12.5, 25, 50, 100, 200(\text{m/s}^2)\}$

(3) Overshoot $\subset \{1, 2, 4, 8, 16(\text{mm})\}$

Furthermore, the stimuli were paired in groups according to size. In other words, for example in the case of the control cycle, displayed stimuli pairs were 4×2 groups $\{10-20, 20-10, 20-40, 40-20, 40-80, 80-40, 80-160, 160-80(\text{ms})\}$. These eight types of stimulus pairs were each tested four times, totaling thirty two tests. The order of three types of experiments was selected randomly and the order of the stimulus pairs displayed in each experiment was also selected randomly (constant method^[16]).

The trajectory of experiment 1 which modified the value of the control command cycle is shown in Fig. 7 (2), the trajectory of experiment 2 which modified the value of the acceleration is shown in Fig. 7 (3) and the trajectory of experiment 3 which modified the value of the overshoot value is shown in Fig. 7(4).

The number of participants in each experiment was 14 participants for the control cycle, 17 participants for acceleration and 10 participants for overshooting. Not including the overlap, there was a total of 29 participants aged between 20–39 years. The length of the experiment including practice and break times was approximately one hour.

It is preferable that haptic devices are capable of displaying the difference threshold specified in this paper for all three parameters. However, it is also preferable that haptic devices with a sufficiently strong motor output are capable of displaying the difference threshold for at least control response cycles, devices with sufficiently short control command cycles are capable of displaying the difference threshold for acceleration and difference threshold are capable of displaying the difference threshold for at least overshooting.

2.4 Experimental results

When participants randomly replied to all the tests in this experiment, the accuracy rate (hereinafter referred to as “chance level”) was 50 percent. In addition, when participants randomly replied to half the tests that were discriminable and half that were not discriminable, the accuracy rate was 75 percent. In this paper, in terms of discrimination being possible for 50 percent or more of the tests, the range of an accuracy rate of 75 percent or more for a stimulus pair is defined as the difference threshold. Furthermore, whether or not there is a significant difference in the accuracy rate of each stimulus pair will be verified as a method of analyzing the experimental results. The average value of the accuracy rate for all participants will be compared for each stimulus pair using the Student's t-test. Stimulus pair groups with a hazard ratio of less than 5 percent will be determined to have a significant difference in the accuracy rate.

The average accuracy rate of all participants will be shown for each stimulus pair. The accuracy rate of stimulus pairs with different control response cycles is shown in Fig. 8, the accuracy rate of stimulus pairs with different acceleration is shown in Fig. 9 and the accuracy rate of stimulus pairs with different overshooting is shown in Fig. 10. The error bar in the figure shows a 95 percent confidence interval for the accuracy rate, the red dashed line shows the accuracy ratio has a 50 percent chance level and the blue dashed line shows the accuracy ratio has a 75 percent difference threshold.

Figure 8 shows that it can be said that it is difficult to discriminate the control response cycle when the control response cycle is smaller than 40 ms as there is no statistically significant difference between the accuracy ratio and the chance level when the control response cycle is less than 40 ms.

On the other hand, the accuracy ratio was 75 percent or more on average when the control response cycle was 40 ms – 80 ms and it can be said that discrimination was possible since the accuracy ratio was significantly higher when the stimulus pair was 10 ms – 20 ms

and 20 ms – 40 ms. Furthermore, the accuracy ratio was 90 percent or more when the control response cycle was 80 ms – 160 ms and it shows that the larger the control response cycle the easier it is to discriminate as there is a significant difference with the accuracy ratio when the control response cycle is 40 ms – 80 ms.

From these results, it is apparent that discrimination is difficult when the control response cycle is less than 40 ms, discrimination is possible for 50 percent or more of the tests when higher than 40 ms and clearly possible when 80 ms or higher. In other words, it can be said that the control response cycle (including deflection) needs to be less than 40 ms when the difference threshold for the control response cycle is 40 ms or higher and an extremely hard object is displayed with the haptic device.

Figure 9 shows that there was no statistically significant difference between the accuracy ratio and the chance level when the acceleration of the stimulus pair was 100m/s² – 200 m/s². However, the accuracy ratio increases when the acceleration of the stimulus pair decreases and discrimination becomes possible in 50 percent or more of the tests when 25 m/s² – 50 m/s² and more than 90 percent when 12.5 m/s² – 25 m/s². Furthermore, since there was a statistically significant difference in all four types of stimulus pairs, it is apparent that discrimination becomes easier to smaller the acceleration of these four stimulus types.

From these results it seems that when the difference threshold of the majority of acceleration tests is 50 m/s² or higher and an extremely hard object is displayed with the haptic device, the acceleration of the contact plate needs to be 50 m/s².

Figure 10 shows that there was no statistically significant difference between the accuracy ratio and the chance level when the stimulus pair overshoot is 1 mm – 2mm. However, the accuracy ratio was significantly higher than the chance level when the stimulus pair overshoot is 2 mm – 4 mm. In addition, discrimination was possible in almost all tests when the stimulus pair is 4 mm – 8 mm and 8 mm – 16 mm.

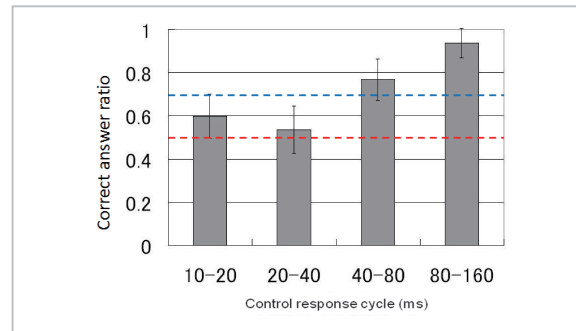


Fig.8 Correct answer ratio for the discrimination of different control response cycle

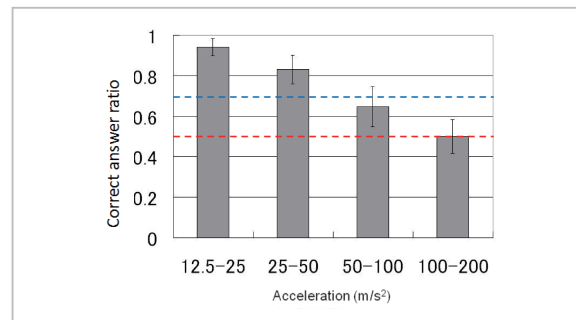


Fig.9 Correct answer ratio for the discrimination of different acceleration

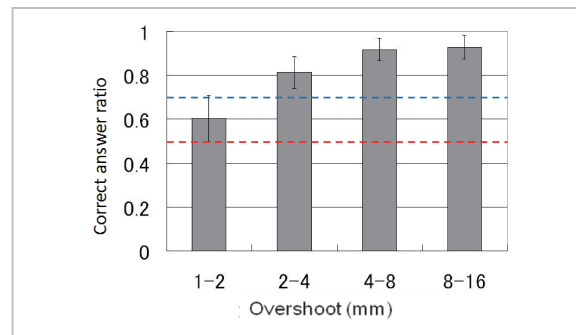


Fig.10 Correct answer ratio for the discrimination of different overshoot

Although there was no significant difference between 4 mm – 8 mm and 8 mm – 16 mm stimulus pairs, discrimination became easier as the overshoot value increased since there was significant difference between 1 mm – 2mm and 2 mm – 4 mm stimulus pairs and 2mm – 4 mm and 4 mm to 8 mm stimulus pairs.

From these results it is apparent that discrimination is difficult in almost all tests when overshoot is less than 2 mm, possible in 50 per-

cent or more tests when 2 mm or higher and possible in almost all tests when 4 mm or higher. In other words, the device overshoot needs to be less than 2 mm when an extremely hard object is displayed with a damping mechanism-type device.

All three experiments produced no worthwhile learning effect since there were not any significant differences in the accuracy ratio in the first sixteen tests and the latter sixteen tests.

2.5 Observations

The experimental results detailed in 2.4 show that it is important to design a haptic device within a new framework that provides the sensation of hardness and has a control response cycle of less than 40 ms, a maximum acceleration capable of displaying 50 m/s² or higher and an overshoot of less than 2 mm.

Most of the current research has focused on experiments involving the control command cycle and the contact plate position calculated by the motor encoder without accurately measuring deflection occurring from the haptic device itself. Consequently, most research does not differentiate between control command cycles and control response cycles nor motor output and the display power to the finger tips.

For example, when positional information was extracted from the motor encoder every 10 ms using the PHANTOM PREMIUM 1.5^[2] and an extremely hard virtual object displayed in a stable manner (stiffness = 1000) was tapped at a 1 m/s speed, 50 ms ~ 60 ms was required from the time of contact with the virtual object until separation and the maximum acceleration at the time of the collision was 15 m/s² ~ 20 m/s². Conversely, when the maximum display power of the PHANTOM PREMIUM 1.5 was 8.5 N, the actual position of the stylus differed to the position calculated by the motor encoder since it deflected^[2] approximately 2.4 mm. As a result, the force and acceleration conveyed to the finger tips through the contact plate cannot be accurately acquired. Positional information can be ascertained with a ±10 μm margin of error even when the display power of the experimental apparatus has the maximum value (236

~ 249 N). Consequently, the control response cycle and maximum acceleration actually acquired as the behavior of the haptic device contact plate has been clarified.

2.6 Examinations and results regarding the weber ratio

Here we will clarify the Weber ratio^[12] ^[16] shown in the stimulus change ratio required for discrimination $\{\Delta I(\text{stimulus change amount})/\Delta I(\text{stimulus amount})\}$ regarding the control response cycle and acceleration using the experimental apparatus. Furthermore, in 2.6, acceleration is shown by the time (hereinafter referred to as “acceleration time”) the finger tip speed changes from -1 m/s to 1 m/s (the 10 ms acceleration time is equivalent to 200 m/s² acceleration).

The control response cycle and acceleration time were provided to participants in the form of three types of standard stimuli and 4 types of comparative stimuli (Table 1 and Table 2).

Two types of stimuli were provided to the participants with three second intervals. One of the two types of stimuli was standard stimulus and the other was comparative stimulus, each provided randomly. The participants replied orally as to whether the first or second was

Table 1 Control stimulus and comparison stimuli for control response cycle

standard stimuli	comparative stimuli			
	+20%	+40%	+60%	+80%
50	60	70	80	90
100	120	140	160	180
150	180	210	240	270

Table 2 Control stimulus and comparison stimuli for acceleration time

standard stimuli	comparative stimuli			
	+20%	+40%	+60%	+80%
60	72	84	96	108
120	144	168	192	216
180	216	252	288	324

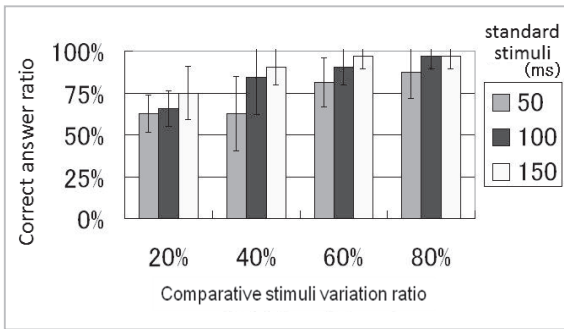


Fig.11 Correct answer ratio for the discrimination of different control response cycle

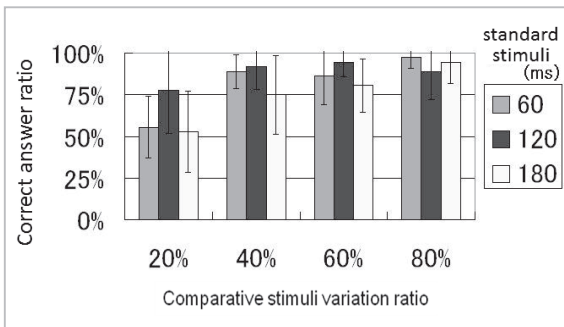


Fig.12 Correct answer ratio for 60, 120, 180 ms standard stimuli acceleration time

harder (short control response cycle/ acceleration time). The results for four 4×3 pattern tests undertaken by eight participants regarding the control response cycle and nine participants regarding acceleration time are shown in Fig. 11 which details the accuracy ratio of all participants regarding the change in the control response cycle and Fig. 12 which details the accuracy ratio regarding the change in acceleration time. The error bar in each Figure shows a 90 percent confidence interval regarding the accuracy ratio.

Figure 11 shows that in regard to the control response cycle the accuracy ratio becomes lower the more the variation ratio of comparative stimuli becomes smaller and discrimination is difficult even in the case of either standard stimuli. When the variation ratio for comparative stimuli was 20 percent, the accuracy ratio in either case was 75 percent or more and when the variation ratio was 60 percent or more, the accuracy ratio in either case was 80 percent or more.

At the same comparative stimuli variation ratio, the shorter the control response cycle for the standard stimulus the lower the accuracy rate becomes. In particular, although the accuracy rate is 80 percent or more when the comparative stimuli variation ratio is 40 percent and the standard stimuli is 100 ms or more, the accuracy rate falls to approximately 60 percent when the standard stimuli is 50 ms. This appears to be a result of the 50 ms control response cycle nearing the difference threshold border line shown in the previous chapter.

These results show that the smaller the comparative stimuli variation ratio the more difficult it becomes to discriminate the control response cycle and the shorter the standard stimuli control response cycle discrimination becomes more difficult when the accuracy ratio is the same. It can therefore be said that the Weber ratio for the control response cycle is 0.2 ~ 0.4 when stimuli is within the difference threshold.

Figure 12 shows the accuracy ratio is 75 percent or more when the comparative stimuli variation ratio is 40 percent or more for acceleration in either case of the standard stimuli. In addition, in either case of the standard stimuli, the accuracy rate was the lowest when the accuracy ratio was 20 percent.

At the same comparative stimuli variation ratio, the accuracy ratio was the highest when the standard stimuli acceleration time was 120 ms. In particular, when the comparative stimuli variation ratio was 20 percent, the accuracy ratio was only 75 percent or more only when the standard stimuli was 120 ms. This shows the possibility that finger tip discriminability is high when acceleration is approximately 120 ms.

These results show that the smaller the comparative stimuli variation ratio, the more discrimination of acceleration time becomes difficult and when the variation ratio is the same, the discriminability is high around 120 ms standard stimuli acceleration time. The Weber ratio for acceleration time appears to be less than 0.2 when standard stimuli is 120 ms and 0.2 ~ 0.4 when the standard stimuli is 60

ms and 180 ms. In other words, when displaying differing hardness on the control response cycle and different acceleration time on haptic devices, it appears that at least an approximately 20 ~ 40 percent difference can be controlled.

3 The development of a haptic device

Here we will discuss the development of a portable haptic device that satisfies the performance detailed in **2** and the creation of a system that extracted the position of the device.

Using the experimental haptic device they created, Tan and the other authors showed through their experiments that the force (terminal force) at the time the feedback force is greatest after holding the object is important for feeling hardness when pinching with the finger tips^[17]. However, most of the existing devices are unable to provide sufficient terminal force in order to display hardness. For example, most of the display power provided by PHANTOM^[2] and SPIDAR^[3] has a maximum of approximately 10 ~ 40 N. In addition, PHANTOM^[2] only has a small maximum acceleration of approximately 15 m/s² and a large maximum overshoot of 2.4 mm or more. Consequently, although the control command cycle is 1 ms, the control response cycle is extremely slow.

In **3**, we will discuss the development of a portable haptic device that provides terminal force sufficient to pinch a virtual object with the thumb and index fingers and satisfies the performance specified in chapter **2**.

3.1 Portable haptic device prototype 1

3.1.1 Outline of prototype 1

Figure 13 shows the pinching part of the initial portable haptic device prototype 1 created and Fig. 14 shows the entire composition. The motor rotation installed in the hand grip part communicates to the ball screw through central gear^[9]. The slider part of the ball screw and the part that the two fingers (thumb and index finger) contact the device (contact plate) are connected by the rigid body made from alu-

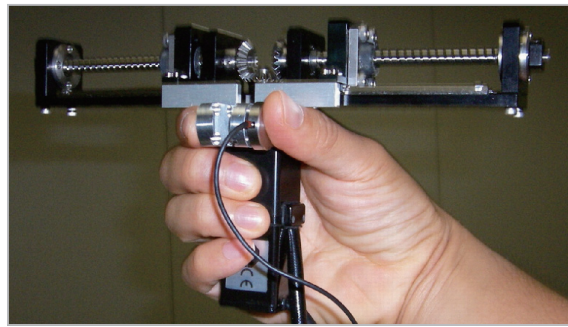


Fig.13 Pinching part of the portable haptic device prototype 1

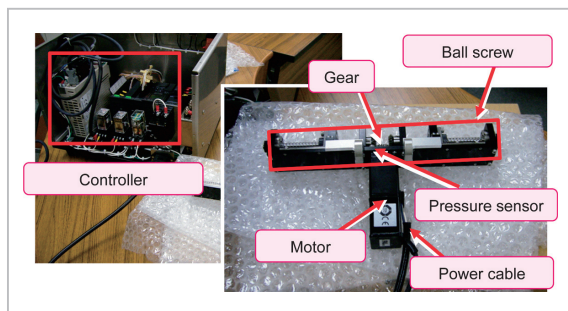


Fig.14 Composition of the portable haptic device prototype 1

minum. A pressure sensor was installed in the contact plate on the thumb side to sense the force applied to the device by the finger (= feedback force the device applies to the finger). An encoder was attached to the motor installed in the device to detect the interval between the two fingers. The motor is controlled by an external controller connected by a cable.

This prototype uses a different control method from that of the PHANTOM and SPIDAR in order to display hard objects. The haptic information displayed by PHANTOM and SPIDAR is a function taking the parameter of the finger tips (or stylus, etc). In other words, the haptic information (output force) is determined by the position of the finger tips. However, in regard to this prototype created by the authors, the position of the finger tips is a function with the parameter of the force added by the finger tips. In other words, the position of the contact plate is determined according to the force applied by the fingers on the device. In many cases, devices such as the PHANTOM

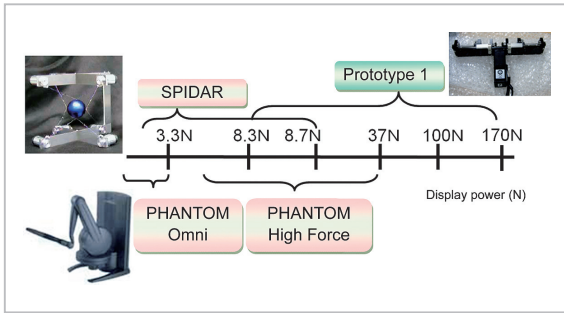


Fig. 15 Comparison of maximum display power

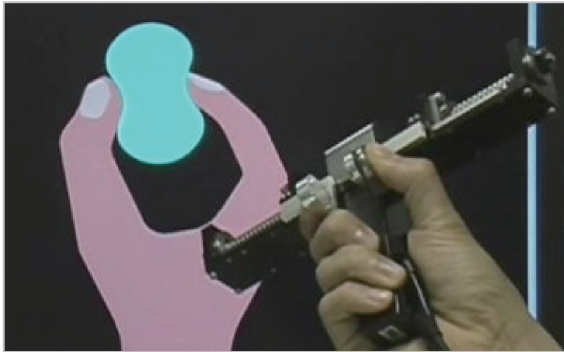


Fig. 16 A user pinching a virtual object simulated by the prototype 1

and SPIDAR use the former method where vibrations occur when hard objects are displayed. The later method used by the prototype provide almost no vibrations even when hard objects are displayed.

The maximum display power that can be displayed on the prototype 1 is each 86 N. This value provides enough feedback force (terminal force) for an average adult male to squeeze with all his strength. In addition, the control command cycle is each 10 μ s, the maximum acceleration when stopped is each 47.9 m/s², and overshoot is each 0.85 mm. The device is 114 mm in length, 220 mm wide and weighs 520 g (not including the cable, etc).

The comparison of display power required to provide hardness is shown in Fig. 15. This Figure shows that the prototype 1 can provide sufficient force in comparison to existing devices such as the PHANTOM and SPIDAR.

3.1.2 Evaluation of prototype 1

Eight participants performed an evaluation as to whether they could recognize the com-

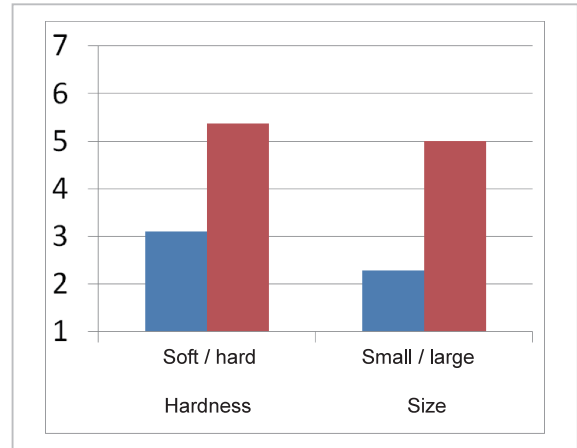


Fig. 17 Average evaluation of subjects for hardness and size

parative difference between the hardness and size of virtual objects using the prototype 1. The monitor used to display images to the participants displayed virtual objects to be pinched by the prototype 1 and an animation of the hand of the participant from the wrist up. The finger movements of the participants, the hand displayed in the monitor and the virtual objects were synchronized by an encoder connected to the prototype 1 motor. Figure 16 shows a participant pinching a virtual object in front of the monitor.

Participants pinched a virtual ball being displayed in the monitor using the prototype 1 and remembered the size and hardness of the displayed object from the sensation of pinching the object. Next, the participants pinched various virtual objects of differing hardness and size using the prototype 1. The participants then compared the virtual objects with first virtual object they remembered and subjectively evaluated the comparative hardness from the following seven stage options. The same test was conducted for the size of the virtual objects for comparative purposes.

<Options for evaluating hardness>

1: Extremely soft/ 2: Soft/ 3: Rather Soft/ 4: The Same/ 5: Rather Hard/ 6: Hard/ 7: Extremely Hard

<Options for evaluating size>

1: Extremely Small/ 2: Small/ 3: Rather Small/ 4: The Same/ 5: Rather Big/ 6: Big/ 7: Ex-

tremely Big

The average replies of the participants for hardness and size of the virtual objects are shown in the test results in Fig. 17. The left side of each graph shows the replies for soft/small objects and the right side of each graph shows the replies for hard/small objects. Since the participants were able to clearly differentiate hardness and size, we were able to verify that the prototype device could display differing hardness and size.

The problems in prototype 1 were the rotation sound of the gears was loud and vibration occurred. In addition, the image displayed in the pinch part could not be seen due to the ball screw between the fingers. As a result we developed prototype 2 to resolve these issues.

3.2 The development of the portable haptic device prototype 2 and 3D image synchronizing system

3.2.1 Outline of prototype 2

The portable haptic device prototype 2 is shown in Fig. 18. In prototype 2, the structure of communicating power from the motor to the ball screw was changed to the gear to a friction wheel in order to cancel sound. In addition, two pressure sensors were attached to the contact plate for both fingers in order to stabilize the system and the field of vision between the two fingers was created by changing the position of the ball screw to the lower part of the motor in order for users to pinch protruding 3D images.

3.2.2 Outline of the 3D image synchronizing system

A 3D image synchronizing system was developed for the purpose of controlling 3D vir-

tual images on a wide screen. This system comprised of an optical motion capture system, a 3D display, a haptic device (prototype 2) and a 3D image display program to be executed on a controlling PC connected to these devices. An overview of the system is shown in Fig. 19 and the system composition is shown in Fig. 20. The details are discussed below.

- Motion capture system

The motion capture system utilizes Radish/3D (2 color cameras). The position of the color marker (Fig. 18) attached to the device is calculated from image information extracted from two cameras installed on both sides of the 3D display. The device positional pose information is obtained from the calculated position of each marker and such information is transmitted to a 3D image display program by a LAN connection. However, the

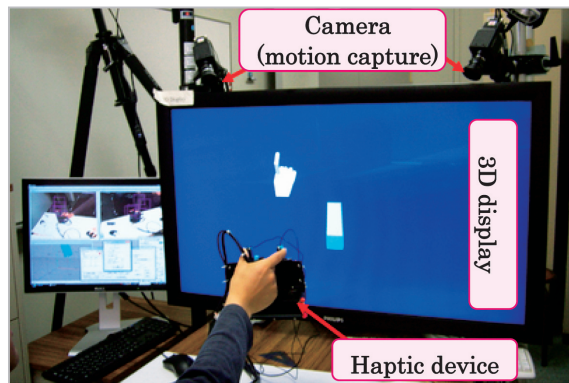


Fig.19 Overview of the 3D image synchronizing system

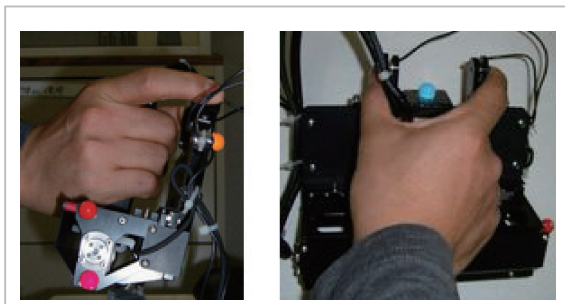


Fig.18 Portable haptic device prototype 2

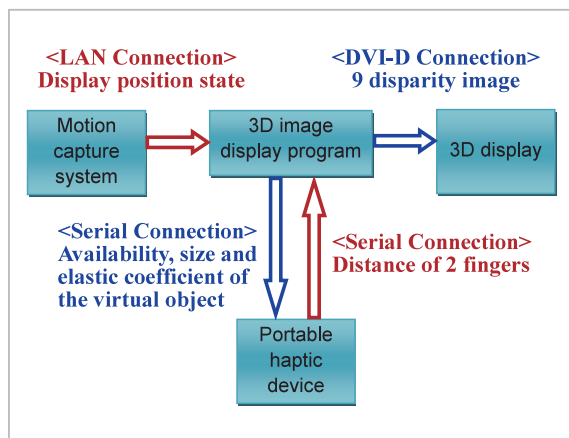


Fig.20 Composition of the 3D image synchronizing system

interval between the two fingers is extracted from the encoder attached to the haptic device motor, not the motion capture system.

-3D display

The 3D display was a Philips glasses-free 3D display (43 inch WOW model: Lenticular type). 3D images are displayed without special glasses by a lenticular lens attached to the display surface.

- 3D image display program

The 3D image display program acquires the six degrees of freedom value which shows the positional pose of the device held by the participant from the motion capture system by a LAN connection and acquires the finger interval value from the device by a serial connection. The size and elastic coefficient is sent to the device when there is a virtual object between the fingers of the participant. However, the device independently controls feedback force and the program receives only the information between the fingers as control results. The virtual objects and the pinching hand in the virtual space are rendered by the OpenGL in the Windows PC based on such information. The displayed images are sent to the 3D display by a DVI-D connection and then displayed in 3D.

- Haptic device

The haptic device used was prototype 2. The size and elastic coefficient of the virtual object is received from the 3D image display program when there is a virtual object between the fingers of the participant. The haptic device controller autonomously calculates the feedback force from the interval between the two fingers and the size and elastic coefficient of the virtual object and haptic information is displayed to the participant. However, the weight of virtual object could not be displayed due to the restrictions of the ungrounded device. Furthermore, the display of weight by ungrounded haptic devices is a future issue that may be possible depending upon the technology that has been filed for patent rights[11].

3.2.3 Issues relating to the 3D image synchronizing system

When the color of the background or

clothes worn by the participant captured by the camera is close to the color marker, the motion capture system utilizing the color marker failed to detect positional information on many occasions. Consequently, a white background was used and participants wore white clothes to stabilize movements. In order to resolve this issue, a Light-emitting diode (LED) was attached to the prototype as a marker and positional information detection failure gradually decreased. However, this in turn resulted in noise occurring when positional information was detected and slight vibrations. The development of a noise cancellation algorithm (filtering) remains an issue that needs to be address in the future.

3.2.4 Subjective evaluation by participants

Six participants used the test system. In this section, we will discuss the subjective evaluations of the haptic device in particular.

- Evaluation of the sensation of size

Participants examined whether size could be recognized by the sense of touch using the haptic device only. Although the size of the virtual objects was the same on the 3D display, the participants gave their responses regarding the size (the thickness of the square prism) of virtual objects which are the same size on the 3D display but have differing feedback force {30, 40, 50, 60(mm)} on the haptic display. As a result, the participants all responded that they could feel the comparative differences in size.

- Evaluation of the sensation of hardness

Participants examined whether hardness could be recognized by the sense of touch using the haptic device only. Although the shape of the virtual objects did not change on the 3D display, the participants gave their responses regarding the hardness of virtual objects which are the same size on the 3D display but have differing feedback force {0.7, 1.5, 3.0, ∞ (N/mm)} on the haptic display. As a result, the participants all responded that they could feel the comparative differences in hardness.

- Evaluation of the sense of control

Participants discussed their impressions of operating the haptic device through a free response format. No respondents were con-

cerned with the sound of the operation. This is thought to be a result of replacing the gear connected to the motor and ball screw that made the most noise on prototype 1 with a friction wheel. However, the transmission of force by the friction wheel did produce a particular vibration (scraping sensation) different from that of the gear. Many participants responded that they were bothered by this vibration. In particular, although the fingers of the participants were floating in space, this vibration occurred up until the time the fingers made contact with the object. Consequently, it is necessary to decrease this vibration caused by the friction wheel. Furthermore, many participants responded that they were concerned with the weight of the device. This was caused by the improvements adding 100g or more weight to the haptic device, amounting to a total weight of over 600 g. The prototype 3 was created to resolve this issue.

3.2.5 Differences in the methods used by participants to discriminate hardness

There were two methods of movement used to verify the hardness of a virtual object using the haptic device. The first method involved participants kneading the haptic device while touching the virtual object with their fingers and determining the force at this time (feedback force type) and the second involved participants determining hardness by the feeling when colliding their fingers with the virtual object (impact type). The distance between the two fingers and the variation of force for each method is shown in Fig. 21 and Fig. 22. The horizontal line shows time (seconds), the vertical line on the left shows the average value of force (N) applied to the device by the fingers and the vertical line on the right shows the interval between the two fingers (mm). The size of the vertical object was 40 mm.

The feedback force type discrimination method shown in Fig. 21 allows participants to determine hardness by applying force to the approximately 40 mm virtual object with their two fingers and feeling the extent their fingers penetrate the object. Most participants used

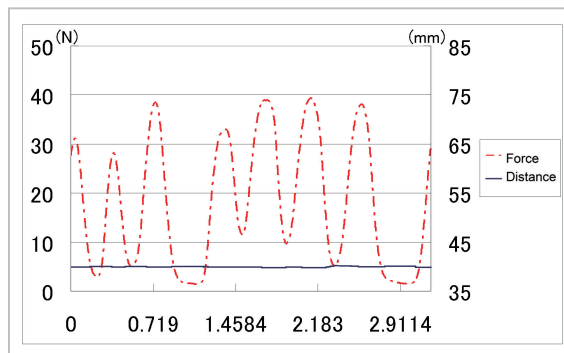


Fig.21 Determination way of hardness using the feedback force

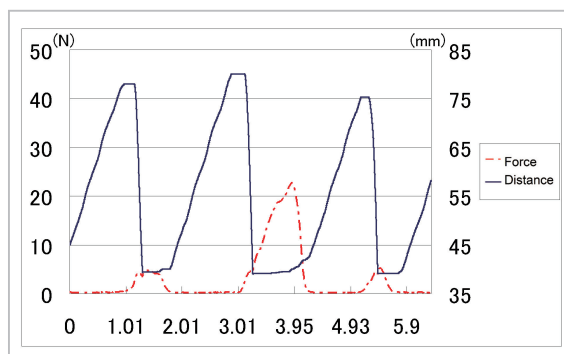


Fig.22 Determination way of hardness using the impact shock

this method to determine hardness.

The impact type discrimination method shown in Fig. 22 allows participants to determine hardness by closing their fingers at a certain speed after separating their fingers from the virtual object and feeling the stationary sensation when colliding with the object. Some participants initially used this method but later used the feedback force type method to discriminate hardness.

When a virtual object has certain level of hardness or more, the interval between the fingers ceases to change even if the pinching force is increased. For example, virtual objects with a spring constant of 40 N/mm can be penetrated only 1 mm even if 40 N of pinching force is applied. Since the feedback force type discriminates the hardness through the pinching force and the depth of the penetration, the discrimination of the hardness of a virtual object with a spring constant of a certain level or more appears to be difficult. On the other hand, al-

though it is possible to discriminate the hardness of a virtual object with a relatively large spring constant using the impact type discrimination method, it is foreseeable that comparing the hardness of a virtual object and real object is difficult even if the difference of the comparative hardness of virtual objects can be discriminated, since the impact sensation of pinching with a haptic device and pinching a real object is not the same.

Furthermore, the maximum value of force applied to the haptic device by participants using either method was approximately 40 N. Most of the desktop haptic devices such as the PHANTOM and SPIDAR cannot provide this amount force. Since it is seemed that normally people output this amount of force when discriminating force, haptic devices need to provide feedback force at this level or higher.

3.3 The potable haptic device prototype 3 and the physical model considering hysteresis

3.3.1 Overview of the prototype 3

In order to reduce the weight of prototype 3, the structure of transmitting force from the motor to the ball screw was changed to force being transmitted from the motor to a wire^[10]. In addition, in order to communicate haptic information, two devices (left hand / right hand) were controlled by one controller. Both devices were 112 mm in length, 115 mm in width and 350g in weight (not including the cable, etc). The two devices minimized communications delay to less than 1 ms by using the same controller. Furthermore, as discussed in the next chapter, a physical model considering hysteresis was created. This enabled users to pinch virtual objects with differing sensations of substances such as glass and clay. The portable haptic device prototype 3 is shown in Fig. 23.

3.3.2 The physical model considering hysteresis

Hysteresis means a “the state of a substance or system relying on the previous passing of events”. For example, clay differs from rubber and even if the applied force returns initial state, the part that has been pushed does not re-

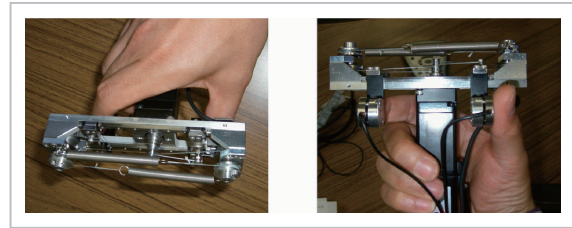


Fig.23 Portable haptic device prototype 3

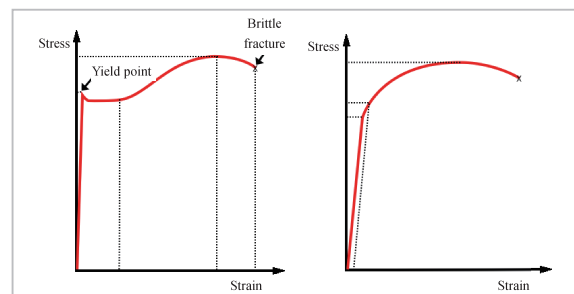


Fig.24 Stress - strain diagram steel (left) and aluminum alloy (right) [18]

turn to its previous shape, the so-called plastic deformation occurs. In other words, the shape of an object relies not only on the force currently applied by also the force applied in the past. In addition, objects such as a ceramic object break before they change shape. This is known as brittle fracture.

For example, Fig. 24 shows the stress and strain of steel and aluminum alloy. As shown in Fig. 24 (left), normally elastic deformation occurs with steel until the yield point. This change of shape is reversible and there is no need to consider hysteresis. However, once the shape has been changed beyond the yield point, the shape is irreversible and hysteresis needs to be considered. Furthermore, although feedback force will not return after the pressure is applied and brittle fracture occurs, this is also irreversible and hysteresis needs to be considered. However, as is the case with the aluminum alloy (Fig. 24 right side), although some materials do not have a distinct yield point, hysteresis needs to be considered in view of plastic deformation occurring when strain increases.

Most existing haptic devices calculate feedback force according to the position of the finger tips (or stylus). At this time, feedback force

is displayed as one function for the penetration distance variable and feedback force output for the virtual object, and when the virtual object is penetrated or returns, the same feedback force is returned provided that it is in the same position. Hysteresis cannot be considered by this type of function. Consequently, plastic deformation and brittle fracture cannot be displayed. For example, the difference in the sensation of rubber (elastic deformation) and clay (plastic deformation) and the difference in the sensation of rubber (elastic deformation) and ceramic objects (brittle fracture) cannot be displayed. A physical model of virtual objects that considers the hysteresis of elasticity, plasticity and brittleness was proposed and installed in the prototype 3.

This research defines the elastic deformation range, plastic deformation range and brittle fracture displacement, and creates models of the elastic range with reversible change, the plastic range with irreversible change and the objects deformed beyond the brittle fracture displacement as broken objects.

For instance, if a virtual object has an elastic deformation range of 5 mm with a spring constant of 10 N/mm, a plastic deformation range of 5 ~ 10 mm with a spring constant of 2 N/mm and a brittle fracture displacement of 20 mm, the feedback force-displacement diagram when the user deforms it by 10 mm and, after releasing it for a time, further deforms by 20 mm in all is shown in Fig. 25. In addition, if the virtual object is 100 mm in length, the dis-

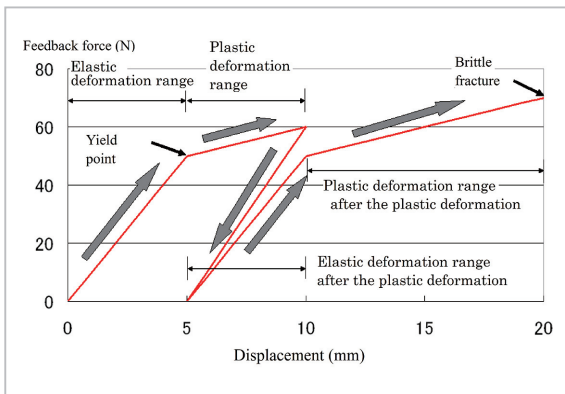


Fig.25 Example of the Stress - strain diagram of virtual object

placed cross-section area 1 mm² and Young's modulus 1 GPa, the deformation value (mm) is equal to the strain value (%) and the feedback force value (N) to the stress values (N/mm²).

It is apparent that most actual materials cannot be expressed by elastic deformation alone but they can be expressed by combinations of elastic deformation, plastic deformation and brittle fracture. For example, a model can be created where rubber has a wide elastic deformation range, clay has a narrow elastic deformation range and a wide plastic deformation range and ceramic objects have a narrow elastic and plastic range and a small brittle fracture displacement.

Most of the existing haptic devices utilize physical models for virtual objects where only elastic deformation occurs but cannot display objects where plastic deformation and brittle fracture occurs. By combining elastic deformation, plastic deformation and brittle fracture, users can pinch various materials and feel the substance.

Most users responded that they could differentiate substances through demonstrations[19] of modeled rubber with only elastic deformation, modeled clay with only plastic deformation and modeled glass with only brittle fracture.

3.3.3 Problems and improvements to prototype 3

The strength of the wires in prototype 3 was a problem. For example, PHANTOM utilizes metal-wire (stranded wire). If the wire shaft radius of metal-wire is small, element wires may break and therefore metal-wire not suited to small-scale devices. Consequently, prototype 3 adopted the fishing line used in de-

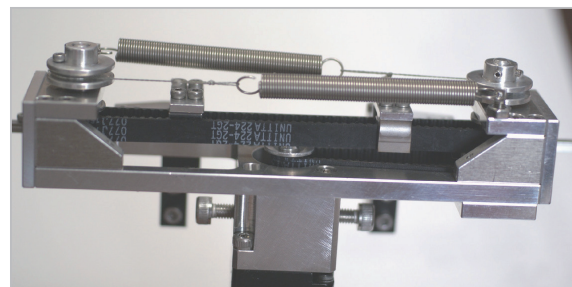


Fig.26 Prototype 3 modified with a toothed belt

vices such as SPIDAR. However, since the prototype provides strong display power, the wire could not be used for a long period of time without breaking. As a result, as shown in Fig. 26, we are currently in the process of developing a prototype modified with a toothed belt.

3.3.4 The impact of delays in haptic information communications

In the real world, haptic information is communicated without delay when two people control one rigid body. However, limited delays occur when communicating with distant locations. Although it is known that audio information communications such as telephones can be interrupted when delays exceed 200 ms, it is not clear what level of delays is acceptable with haptic information communications.

Research has also been conducted on haptic information delays when both haptic information and image information are displayed on existing haptic devices[20]. The impact of delays can be ignored for one way transmissions. However, the impact of delays is large when sharing haptic information with distant locations. For example, consider the scenario where one person is pushing on the right side of a rigid body to the left and another person is pushing on the left side of the rigid body to the right on a system with a 100 ms delay. From the perspective of the person on the left, such person is able to push to the right because the right side was not being supported 100 ms in the past. Similarly, the person on the right is able to push to the left. As a result, the rigid body will greatly shrink after 100 ms. In addition, since the length of the shrunken rigid body will not return even if the other person's force is outputted as the same size of feedback force, a stronger force needs to be returned on both sides. As a result, control becomes unstable, the device will vibrate unnaturally and the user will be disrupted.

Even if the control cycle is 1 ms, haptic information from long distances cannot be communicated in such a short time. In order to examine the level of delays acceptable to the human cognitive mechanism, it would be effective to conduct psychophysical experiments

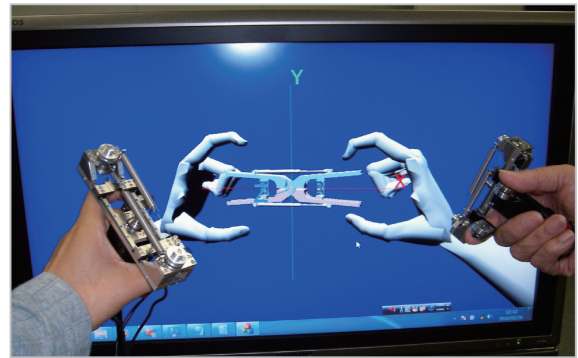


Fig.27 Content example of Haptic communication

with various lengths of delays using multiple haptic devices with a delay small enough not to be noticed by people. However, this has not been possible because the delays on existing haptic devices are too large.

The time required to communicate haptic information between devices can be limited on the proposed haptic device to less than 1 ms by simultaneously controlling two haptic devices with one controller. Specifically, the controller extracts the values shown by the four pressure sensors that are two by two mounted on the two haptic devices, and keeps these two haptic devices simultaneously under a 1 ms cycle. In other words, based on the values shown by the pressure sensors of one haptic device, the other haptic device can be controlled by a delay of 1 ms or lower. Consequently, for instance, when controlling the "sum" of the distance between the two finger tips on the two devices held in the both hands to be constant, one can experience handling with their right hand the right side and by their left hand the left side of a chop-stick being supported by someone as if it were the sensation of a teeter-totter (Fig. 27). In addition, when controlling the "ratio" between the two finger tips to be constant, one can experience holding and handling the right edge of scissors with their right hand and the left edge with their left hand. We plan to set communication delay between these two devices up randomly as 1 ms ~ 1000 ms and determine the amount of acceptable communication delays in the psychophysical experiments.

4 Conclusion

This research addressed the clarification of the cognitive mechanism of hardness and the development of portable haptic devices in order to achieve high presence communications not only by seeing/ hearing/ smelling, but also by “touching”. By clarifying the limits of hardness cognizable to humans, we have defined the device performance required for haptic devices to display hard objects. Furthermore, we developed a portable haptic device that can display sufficiently hard haptic information cognizable to humans and enable users to pinch and operate a virtual object displayed on a large-scale 3D display.

Future issues on clarifying discriminability of hardness are to be discussed. The present study explained the cognitive mechanism of hardness in the experiments where hardness is discriminated only from the haptic information without providing the visual and audio information. Hereafter, it is also necessary to determine how the haptic information can discriminate hardness in the multimodal environment where the visual and audio information is simultaneously displayed. Also, in regard to the haptic information communication through multiple haptic devices, there have been so far no sufficient experiments. The improvement of the prototype 3 described in the preceding chapter is supposed to create an environment where such experiments can be put into prac-

tice. For the future, we hope to successfully share the haptic information with remote locations, which is considered to be extremely difficult at the present day.

Future issues on the portable haptic device are to be specified. The motor part accounts for approximately 200 g of the prototype 3 totaling 340 g in weight, due to which drastic weight saving is difficult with the current display power secured. Also, since most of 115mm wide prototype is used for the finger tips stroke, any further miniaturization appears to be implausible. In other words, we consider it is difficult that size and weight of the portable haptic device reduce. Conversely, it can be said that there is a great possibility for creating contents for synchronizing 3D images and for improving the motion capture system. We hope to contrive useful content that enables the user to recognize its hardness by pinching virtual objects. Furthermore, a method that enables stable and steady extraction of the positional information of the device not using optical motion capture systems but using mechanical systems such as the PHANTOM can also be formulated. Hereafter, we aim that ultra realistic communication technologies involving “seeing/ hearing/ smelling/ touching” be more generally utilized based on the study results of our research group.

This research is supported in part by Grants-in-Aid for Scientific Research (Kiban-B, No. 21300088).

References

- 1 NICT press release: <http://www2.nict.go.jp/pub/whatsnew/press/h20/080930/080930-3.html>, Sep.30, 2008.
- 2 SensAble Technologies, Inc: Haptic Devices, <http://www.sensable.com/products-haptic-devices.htm>.
- 3 K. Akahane, S. Hasegawa, Y. Koike, and M. Sato, The high definition haptic controller which realizes update cycles higher than 10khz. Transactions of the virtual reality society of Japan, Vol. 9, No. 3, pp. 217–226, 2004.
- 4 Kimura, A. Uesaka, F. Shibata, and H. Tamura, Function Design and Evaluation of Tool Device Facilitating Pick and Move Manipulation in Spatial Works, Vol. 51, No. 2, pp. 314–323, 2010.
- 5 K. Nakayama, C. Oshima, and H. Ando, Investigation of haptic device requirements for hard object rendering, The Transaction of Human Interface Society, Vol. 12, No. 2, pp. 129–138, 2010.
- 6 K. Nakayama, J. Liu and H. Ando, Investigation of hardness perception for haptic device development,

Special Issue of International Journal of Biometrics (accepted with under modifications).

- 7 K. Nakayama and N. Inoue, Cognitive experiments on human sense of hardness discriminability, Proceedings of The Second International Workshop on Kansei 2008, pp. 90–93, 2008.
- 8 K. Nakayama and N. Inoue, Weber ratio and difference threshold for hardness perception, Proceedings of The 11th International Conference on Humans and Computers, pp.127–132, 2008.
- 9 K. Nakayama and N. Inoue, Portable haptic device, application for a patent (Japan), application number: 2008–274297, 2008.
- 10 K. Nakayama, Portable haptic device, application for a patent (Japan), application number: 2009–196874, 2009.
- 11 K. Nakayama, Non-grounded portable haptic device, application for a patent (Japan), application number: 2009–207062, 2009.
- 12 E. H. Weber: De pulsu, resorptione, auditu et tactu, Annotationes anatomicas et physiologicae, Leipzig, 1834.
- 13 H. Hoshino and S. Tachi, A Method to Represent an Arbitrary Surface in Encounter Type Shape Representation System, Transactions of the Virtual Reality Society of Japan, Vol. 4, No. 2, pp. 445–454, 1999.
- 14 S. Kikuchi and K. Hamamoto, Development of Haptic Display Actuated with Magnetorheological Fluid and Artificial Muscle (HAMA Device), The transactions of the Institute of Electrical Engineers of Japan. C, Vol. 129, No. 10, pp.1859–1864, 2009.
- 15 S. S. Stevens, On the psychophysical law, Psychological Review, Vol. 64, No. 3, pp. 153–181, 1957.
- 16 Y. Tanaka, Psychological measurement, University of Tokyo Press, 1977.
- 17 H. Z. Tan, N. I. Durlach, G. L. Beauregard, and M. A. Srinivasan, Manual discrimination of compliance using active pinch grasp: The roles of force and work cues, Perception and Phychophysics, Vol. 57, No. 4, pp. 495–510, 1995.
- 18 Wikipedia: <http://ja.wikipedia.org/>
- 19 K. Nakayama, C. Oshima, and H. Ando, Haptic Rendering of Elastic / Plastic / Brittle material with Short Delay Communication, Interaction 2010, 2010.
- 20 H. Ohnishi and K. Mochizuki, Psychophysical Measurement of Effect of Delay of a Haptic Display on Perception of Elastic Force, IEICE Technical Report, Vol. 106, No. 495(CQ2006-81), pp. 11–16, 2007.

(Accepted Sept. 9, 2010)



NAKAYAMA Koichi, Ph.D.
*Guest Researcher, Multimodal
Communication Group, Universal
Media Research Center/Associate
Professor, Graduate School of Science
and Engineering, Saga University*
*Portable Haptic Device, Optimization
Algorithm, Artificial Intelligence*



ANDO Hiroshi, Ph.D.
*Group Leader, Multimodal
Communication Group, Universal
Media Research Center*
*Brain and Cognitive Sciences,
Multisensory Cognition Mechanisms,
Multisensory Interfaces*